Biomedicine & Pharmacotherapy 175 (2024) 116719

Contents lists available at ScienceDirect

Biomedicine & Pharmacotherapy

journal homepage: www.elsevier.com/locate/biopha

Evaluation of BH3 mimetics as a combination therapy with irradiation in head and neck squamous cell carcinoma

Katja Korelin [a,b,*], Mayke Oostveen [a], Wafa Wahbi [a,b], Filipp Ianevski [c], Bruno Cavalcante [a,d,e], Laura Turunen [c], Ilya Belevich [f], Ahmed Al-Samadi [a,b,g], Tuula Salo [a,b,h,i,j]

[a] Department of Oral and Maxillofacial Diseases, University of Helsinki, Helsinki 00014, Finland
[b] Translational Immunology Research Program (TRIMM), University of Helsinki, Helsinki 00014, Finland
[c] Institute for Molecular Medicine Finland (FIMM), University of Helsinki, Helsinki 00290, Finland
[d] Gonçalo Moniz Institute, Oswaldo Cruz Foundation (IGM-FIOCRUZ/BA), Salvador 40296-710, Brazil
[e] Department of Pathology and Forensic Medicine, School of Medicine, Federal University of Bahia, Salvador 40110-909, Brazil
[f] Electron Microscopy Unit, Institute of Biotechnology, Helsinki Institute of Life Science, University of Helsinki, Helsinki 00014, Finland
[g] Institute of Dentistry, School of Medicine, Kuopio Campus, University of Eastern Finland, Kuopio, Finland
[h] Cancer and Translational Medicine Research Unit, University of Oulu, Oulu 90014, Finland
[i] Medical Research Center, Oulu University Hospital, Oulu 90220, Finland
[j] Department of Pathology, Helsinki University Hospital (HUS), Helsinki 00029, Finland

ARTICLE INFO

Keywords:
Head and neck squamous cell carcinoma
BH3 mimetics
Combination therapy
A-1155463
A-1331852
Navitoclax
High-throughput drug combination screen
Apoptosis assay
Clonogenic survival assay
Invasion assay
Xenograft

ABSTRACT

Introduction: Head and neck squamous cell carcinoma (HNSCC) is a common cancer with a five-year survival rate around 60%, indicating a need for new treatments. BH3 mimetics are small molecules that inhibit anti-apoptotic Bcl-2 family proteins, resulting in apoptosis induction.

Methods: We performed a high-throughput screen using a Myogel matrix to identify the synergy between irradiation and the novel BH3 mimetics A-1155463, A-1331852, and navitoclax in 12 HNSCC cell lines, normal (NOF) and cancer-associated fibroblasts (CAF), and dysplastic keratinocytes (ODA). Next, we examined synergy in an apoptosis assay, followed by a clonogenic assay and a Myogel spheroid on selected HNSCC cell lines. Finally, we applied zebrafish larvae xenograft to validate the effects of navitoclax and A-1331852.

Results: All three BH3 mimetics exhibited a strong synergy with irradiation in eight HNSCC cell lines and ODAs, but not in NOFs and CAFs. A-1155463 and A-1331852 induced apoptosis and reduced proliferation, and together with irradiation, significantly increased apoptosis and arrested proliferation. A-1331852 and navitoclax significantly decreased the clonogenicity compared with the control, and combination treatment led to a decreased clonogenicity compared with monotherapy or irradiation. However, unlike navitoclax or A-1155463, only A-1331852 significantly reduced cancer cell invasion. Furthermore, in spheroid and zebrafish, irradiation appeared ineffective and failed to significantly increase the drug effect. In the zebrafish, A-1331852 and navitoclax significantly reduced the tumor area and metastasis.

Conclusions: Our findings encourage the further preclinical investigation of BH3 mimetics, particularly A-1331852, as a single agent or combined with irradiation as a treatment for HNSCC.

1. Introduction

Head and neck squamous cell carcinoma (HNSCC) is the sixth most common cancer worldwide [1]. Despite improved treatments, the survival rate has remained stagnant at approximately 60% [2]. Treatment approaches for HNSCC include surgery combined with radio-, chemo-, immuno-, or targeted therapy. Current chemotherapeutic agents are nonselective and accompanied by severe side effects, especially when combined with radiotherapy. Furthermore, newer therapeutic approaches in HNSCC, targeted therapy (cetuximab), as well as the immunotherapeutic PD-1 inhibitors (nivolumab and pembrolizumab) have low response rates and rapidly lead to drug resistance. Therefore, new molecular-targeted therapies are urgently needed for integration with existing treatment regimens.

* Corresponding author at: Department of Oral and Maxillofacial Diseases, University of Helsinki, Helsinki 00014, Finland.
E-mail address: katja.korelin@helsinki.fi (K. Korelin).

https://doi.org/10.1016/j.biopha.2024.116719
Received 7 March 2024; Received in revised form 2 May 2024; Accepted 6 May 2024
Available online 15 May 2024

Radiotherapy is an effective treatment against cancer; however, resistance remains a clinical problem [3]. One of the suggested mechanisms of resistance to anticancer treatments is an alteration in the expression of B-cell lymphoma-2 (Bcl-2) family members. The Bcl-2 family consists of three groups based on their functions: pro-apoptotic BH3 only proteins, anti-apoptotic proteins (Bcl-2, Bcl-xL, and Mcl-1), and pro-apoptotic pore formers (BAX/BAK) [4]. Bcl-2 family proteins control cell death by regulating the mitochondrial membrane permeability via BAX/BAK proteins, allowing the release of cytochrome c to the cytoplasm and caspase activation, leading to apoptosis [4]. In HNSCC, the Bcl-2 protein is not normally upregulated; it can be overexpressed in around 15–25% of HNSCC tumors [5,6]. However, the Bcl-xL protein appears to be consistently upregulated, rendering it an attractive therapeutic target [5,7]. Furthermore, a high Bcl-xL expression in the tumor area has correlated with the presence of lymph node metastases and decreased survival in oropharyngeal and tongue cancer patients [8,9].

BH3 mimetics are small molecules that mimic BH3 proteins by binding to anti-apoptotic Bcl-2 family proteins [5]. Six BH3 mimetic compounds (A-1210477, A-1331852, ABT-737, navitoclax, S63845, and venetoclax) have been studied in HNSCC, with the most validated reportedly capable of inducing apoptosis (*in vitro*) and tumor growth inhibition (*in vivo*) as a single agent or in combination therapies [5]. As a selective Bcl-2 inhibitor, venetoclax has been approved by the US Food and Drug Administration (FDA) for patients with acute myeloid and chronic lymphocytic leukemia [10]. Several clinical trials have been conducted or are ongoing on navitoclax in the treatment of leukemia and solid tumors [11] (https://clinicaltrials.gov/). However, no ongoing clinical trials investigating the effects of any BH3 mimetic drugs on HNSCC exist.

A recently published high-throughput screen has identified effective and synergistic drug–irradiation combinations using a compound library (n = 396) and ionizing irradiation on HNSCC cells cultured on a human leiomyoma–derived matrix, Myogel [12]. This screen identified a BH3 mimetic drug, the Bcl-2/Bcl-xL inhibitor navitoclax, as the most synergistic combination with irradiation. Navitoclax exhibited synergy when combined with irradiation in all 13 HNSCC cell lines tested, indicating its therapeutic potential for HNSCC patients [12].

To date, only a few publications have investigated selective Bcl-xL inhibitors in HNSCC. One study reported that the Bcl-xL inhibitor A-1155463 eliminated cisplatin-induced senescent HNSCC cells [13], while another study combined A-1331852, a re-engineered version of A-1155463, with another targeted treatment, the Mcl-1 inhibitor S63845 [7]. In that report, this combination induced apoptosis in HNSCC cell lines and tumor tissue explants and reduced the tumor burden in zebrafish xenografts [7].

In this study, we further investigated the anticancer effects of promising BH3 mimetics (navitoclax, A-1155463, and A-1331852) as a single agent and when combined with irradiation in several *in vitro* assays and an *in vivo* model. We performed a high-throughput screen (HTS) dose–response matrix analysis of 11 locally established HPV-negative HNSCC cell lines, one commercial tongue metastatic carcinoma cell line (HSC-3), HPV-16 transfected dysplastic keratinocytes (ODA), and normal (NOF) and cancer-associated fibroblasts (CAF) to validate the effectiveness, selectivity, and synergy between BH3 mimetics and irradiation. The apoptosis assay using two HNSCC (UT-SCC-40 and UT-SCC-42A) cell lines confirmed that both Bcl-xL inhibitors substantially induced irradiation-associated apoptosis. A spheroid invasion assay revealed that A-1331852 significantly reduced HNSCC cell invasion as a single agent and in combination with irradiation. Finally, we applied an *in vivo* zebrafish larva model to validate the anticancer effects of BH3 mimetics (navitoclax and A-1331852) as single agents and in combination with irradiation in UT-SCC-42A cells. In zebrafish larvae, both BH3 mimetics, particularly A-1331852, significantly reduced the HNSCC tumor area and metastasis.

2. Materials and methods

2.1. Cell lines

For HTS, we used a total of 15 cell lines including 12 HNSCC cancer cell lines, HPV16-immortalized mucosal keratinocytes (ODA) [14], NOF [15], and CAF [16]. We used 12 HPV-negative HNSCC cell lines taken from different sites of the head and neck area (Table S1). Among these, eight of the cell lines were established at Turku University Hospital (the Department of Head and Neck Surgery, Turku, Finland), three cell lines were locally established in the Department of Oral and Maxillofacial Diseases at the University of Helsinki (Helsinki, Finland) using the protocol by Tuomainen K *et al.* [12], and one commercially available metastatic tongue cancer cell line (HSC-3, Japan Health Sciences Foundation, Japan). Locally established HNSCC cell lines were cultured in a minimal essential medium, supplemented with L-glutamine (2 mmol/l), 10% fetal bovine serum (FBS), and a nonessential amino acid solution (from Thermo Scientific, Massachusetts, USA). ODA were cultured in a Keratinocyte–SFM Medium (Kit) with L-glutamine, EGF, and BPE (Gibco). Fibroblasts (NOF and CAF) were cultured in Ham's Nutrient Mixture F-12 with 1% L-alanyl-L-glutamine (DMEM/F-12 1:1 GlutaMAX) supplemented with 10% FBS. The HSC-3 cell line was cultured in DMEM/F-12 (Gibco) supplemented with 10% FBS. All cell culture media were supplemented with penicillin (100 U/ml), streptomycin (100 µg/ml), and 250-ng/ml amphotericin B (all from Thermo Scientific). Cell lines were tested for mycoplasma using the EZ-PCR Mycoplasma Detection Kit (Biological Industries, Sartorius, Göttingen Germany).

2.2. High-throughput combination screen

We used drug sensitivity and resistance testing (DSRT) adapted from a previously published protocol for leukemia cells [17]. DSRT was conducted at the High-Throughput Biomedicine Unit (HTB) at the Institute for Molecular Medicine Finland (FIMM). All prospective liquid handling was performed using an automated reagent dispenser (BioTEK, MultiFlo™ FX, Winooski, Vermont, USA).

We performed DSRT on 15 cell lines (12 HNSCC cancer cell lines, NOF, CAF, and ODA) cultured in 384-well plates (Corning, NY, USA) coated with Myogel (0.5 mg/ml) [18]. Myogel was used to provide the tumor microenvironment for cancer cells, which reportedly improves the predictability of drug testing [19]. Myogel was diluted in a serum-free medium (0.5 mg/ml) and applied to plates (5 µl/well) using an automated reagent dispenser and placed in an incubator. On the following day, cells were detached using trypsin/EDTA (Thermo Scientific), diluted to the appropriate culture medium and seeded onto plates using the automated reagent dispenser (500 cells in 20 µl/well). Following overnight incubation, the BH3 mimetics (A-1155463, A-1331852, and navitoclax) and reference treatment cisplatin were added to the plates using an ultrasound dispenser (Echo 550, Labcyte, San Jose, CA, USA) in five tenfold concentrations (1–10 000 nM) in triplicate (Table S2). The compounds were dissolved in dimethyl sulfoxide (DMSO) except cisplatin, which was dissolved in water due to stability issues. Each cell line was screened using five parallel compound sets. Each set was irradiated three hours after compound administration at different doses (0, 1, 2, 4, or 8 Gy). The radiation source was the gamma irradiator OB29/4 (STS, Braunschweig, Germany, isotope Cs137) at the dose of 0.0193 Gy/s. After three days, the CellTiter-Glo 2.0 (CTG) luminescent cell viability assay (Promega, Madison, WI, USA) was used to determine the cell viability. CTG (25 µl/well) was added onto the plates using a reagent dispenser and placed on a rocker platform for 5 min at 450 rpm. The plates were centrifuged for 5 min at 1000 rpm at RT and the luminescence was detected using the Pherastar reader (BMG LABTECH GmbH, Ortenberg, Germany). For the following studies, the apoptosis, spheroid, and zebrafish assays, the highest radiation dose (8 Gy) was selected since it possessed the greatest synergistic effect with

the drugs.

2.3. Drug sensitivity score analysis

To quantitatively profile the effects of the compounds, we calculated the drug sensitivity score (DSS) using the Breeze software (available at https://breeze.fimm.fi) [20]. DSS combines several parameters (IC50, the curve slope, and the minimum and maximum responses) into a single metric [17]. In order to calculate the dose–response curves, the compound effect was normalized against negative (0.1% DMSO) and positive (100-μM Benzethonium Chloride, BzCl) controls.

2.4. Dose–response matrix analysis and synergy scores

To test whether the compound–irradiation combinations acted synergistically or antagonistically, we compared the observed responses to the expected combination responses. We then calculated the treatment responses and generated the dose–response matrices and calculated the ZIP synergy score using the ZIP reference model with the SynergyFinder web application (version 3.0; https://synergyfinder.fimm.fi) [21]. Based on the ZIP synergy score, combinations were classified as synergistic, antagonistic, or noninteractive. Combinations with a score exceeding 10 were considered synergistic and those under −10 as antagonistic. Scores between −10 and 10 were considered noninteractive combinations.

2.5. Apoptosis assay

The assay was performed for two HNSCC cells lines (UT-SCC-42A and UT-SCC-40) to detect the apoptotic effects of A-1155463 and A-1331852 with or without irradiation (8 Gy). Cancer cells were irradiated three hours after compound exposure with 8 Gy. In each experiment, two tissue culture–treated 96-well plates (Corning) were coated with 50-μl Myogel (0.5 mg/ml) diluted using a serum-free culture medium and left in an incubator overnight. On the following day, the excessive Myogel coating was removed from the wells. Cells were labeled with CellTrace Far Red dye (Invitrogen, Carlsbad, CA, USA) following the manufacturer's instructions, seeded on to the coated plates (100 μl, 2000 cells/well), and left to adhere overnight in the incubator. On the following day, the culture medium was replaced with a culture medium containing the BH3 mimetics (A-1155463 and A-1331852; 10, 100, or 1000 nM) and the IncuCyte Caspase-3/7 Apoptosis Assay Reagent (2.5 μM; Sartorius) for apoptosis detection. After compound administration, cells were placed in the Incucyte S3 live cell analysis system (Sartorius) and imaged every three hours over three days. Three hours after drug exposure, one of the two plates was irradiated with 8 Gy. Cancer cell proliferation (red object count), the number of apoptotic cells (green object count), and the ratio of apoptotic cells were measured (red and green objects divided by red objects) using the Incucyte software. UT-SCC-42A cells were only analyzed up to day two due to their rapid proliferation and, thus, the fading dye. All experiments were repeated four times using three replicates.

2.6. Clonogenic survival assay

For the clonogenic survival formation assays, a defined number of cells were exposed to three different doses of compounds (A-1331852 or navitoclax) and/or irradiation (2 Gy) and incubated for up to 7 days. For the clonogenic assay, only 2 Gy was applied because an 8-Gy dose was too lethal for the cells in low-density two-dimensional (2D) cultures. Two representative cell lines, UT-SCC-42 and UT-SCC-40, were seeded on 24-well plates in triplicate. Cell colonies were fixed using ice-cold methanol for 5 min and stained with 0.2% crystal violet for 15 min, then imaged with the Cell3iMager (Screen, Kyoto, Japan) plate scanner and manually analyzed using the "cell counter" tool of Image J (National Institutes of Health, USA). The results represent the average of three separate experiments, and the plating efficiency (PE) for the untreated controls and surviving fraction (SF) were determined using the following formulas: PE = [# of colonies formed/# of cells seeded] and SF = [# of colonies formed/(# of cells seeded × PE)].

2.7. Spheroid invasion assay

We applied the *in vitro* spheroid assay to determine the cancer cell invasion properties [22]. To create round spheroids, laryngeal carcinoma (UT-SCC-42A) cells (45 μl, 1000 cells/well) were seeded on to two U-shaped ultra-low attachment 96-well plates (Corning). After spheroid formations over four days, spheroids were treated with three different concentrations of BH3 mimetics (5-μl navitoclax/1155463/A-1331852). After three hours, one of the two plates was irradiated with 8 Gy after three hours after compound exposure. After irradiation, both plates were embedded in a Myogel–fibrin mixture (1.0 mg/ml, 50 μl/well), resulting in a final concentration of 0.5 mg/ml in the well. The Myogel–fibrin mixture was prepared using the following concentrations: 1.0-mg/ml Myogel, 1.0-mg/ml fibrinogen (Merck, Darmstadt, Germany), 0.67-U/ml thrombin (Merck), and 66.67-μg/ml aprotinin (Merck). After gel addition, the plates were left in an incubator for 30 min to ensure proper gelation of the matrix. Next, the culture medium–containing drugs were added on top of the gels. Plates were imaged daily for three days with an inverted microscope (Nikon Eclipse TS100, Tokyo, Japan). All experiments were repeated four times in six replicates.

The cancer cell invasion area and maximum invasion length were analyzed using an open-source microscopy image browser (MIB) (version 2.84; http://mib.helsinki.fi/) [23]. First, we performed manual segmentation of the spheroid and invasion area of 126 representative images out of the 1920 total images (6.6%). A 50-layer deep convolutional neural network (DeepNetV3 Resnet50) [24] was trained using the DeepMIB tool [25] with representative images to recognize the invasion and spheroid area (Fig. S1), following the prediction of the full image set to generate segmentation models for each image. Prediction was performed with 10% overlapping tiles to minimize edge artifacts, and the quality of the prediction model was evaluated using a manual check. The settings for training are presented in Supplementary Figure S1b. The analysis of the invasion area and length was performed using a recent version of MIB (version 2.84-beta). The total area of the spheroid and the cancer cell invasion were extracted using the "Count labels" tool of DeepMIB in pixels and converted to physical units for comparative analysis. The models were filtered using the Distance Map filter to calculate the distance of each pixel in the invasion area to the spheroid area using the Euclidean distance transformation. The length of the furthest invasion point to the edge of the spheroid (max distance) was extracted using the "Get statistics" tool of MIB.

2.8. Zebrafish larvae assay

Before the actual assay, we performed a cytotoxicity test using compounds and irradiation separately and in combination to confirm the safety of the compounds for the fish. We applied this model to test the efficacy of the combination of navitoclax or A-1331852 with irradiation on HNSCC cells (UT-SCC-42A) labeled with CellTrace Far Red and injected in the perivitelline space of the zebrafish larvae. The zebrafish larvae were kept at 34°C in an embryotic medium (Merck). We used wild-type zebrafish (Danio rerio) larvae (from the AB strain) at 2 dpf. The fish were dechorionated, and anesthetized with 0.04% Tricaine before the perivitelline space microinjection of 4 nl of a cell suspension (1500 cells/fish).

After injection, fish were transferred to the 24-well plates, 1000-μl fresh embryonic medium containing compounds were added to the wells (1000-nM navitoclax, 1000-nM A-1331852). Three hours after compound administration, fish were irradiated with a single 8-Gy dose. After three days, fish were fixated with 4% paraformaldehyde overnight and mounted on slides. Fish were imaged under a fluorescence microscope

Nikon Ti-E and the tumor area was measured using Image J. Cancer cells that had invaded from the main tumor in the abdomen towards other parts of the fish, such as the caudal or head region, were considered metastasis (Fig. S2). Imaging was performed at the Biomedicum Imaging Unit at the University of Helsinki (Helsinki, Finland), with support from Biocenter Finland. Each treatment group included 58–67 individual fish.

2.9. Ethics approvals

The use of human leiomyoma tissue was approved by the Regional Ethics Committee of the Northern Ostrobothnia Hospital District (statement number 2/2017), and all studies were performed in accordance with the relevant regulations

Cancer samples for establishing the HNSCC cell lines (UH-SCC-17A, UH-SCC-17A, and UH-SCC-18A) were collected in this study according to our institutional Research Ethics Board approval (Regional Ethics Committee of Northern Ostrobothnia Hospital District, statement number 31/2016).). Patient participation was voluntary and required informed consent.

In vivo experiments were conducted at the Zebrafish Unit of the University of Helsinki (Helsinki, Finland) adhering to the ethical permission (ESAVI/13139/04.10.05/2017) granted by the regional state administrative agency.

2.10. Statistical analysis

Statistical analyses were performed using SPSS (version 29.0; IBM Corp., Armonk, NY, USA) and GraphPad Prism 9 (Dotmatics, San Diego, CA, USA) software packages. To determine the statistical significance of the apoptosis assay and clonogenic survival assay, we performed a two-way analysis of variance (ANOVA) followed by the Tukey test. For the spheroid assay, we applied a one-way ANOVA followed by the Tukey test to determine statistical significance. For the zebrafish larvae, statistical differences in the tumor area were determined using a one-way ANOVA with the Bonferroni correction; for the metastasis percentage, the Wald Z test for the independent proportion with FDR p-value adjustment was used to identify significant differences; finally, confidence intervals were calculated using the Wilson score. Statistical significance was set to $p < 0.05$. We present the following p values: $^{*}p < 0.05$, $^{**}p \leq 0.01$, $^{***}p \leq 0.001$, and $^{****}p \leq 0.0001$.

3. Results

3.1. High-throughput combination screen reveals synergistic effects of BH3 mimetics in combination with irradiation in HNSCC cells, whereas noninteractive effects observed in fibroblasts

To validate the synergistic and selective effects of Bcl-xL inhibitors (A-1155463 and A-1331852), alongside navitoclax, we applied a 6 × 5 dose–response matrix analysis by applying five tenfold drug concentrations (1–10 000 nM) and four irradiation doses (1–8 Gy) on 12 HNSCC cell lines, dysplastic keratinocytes (ODA), NOF, and CAF. For comparative purposes, the screen also included cisplatin as a control treatment.

We found that navitoclax and the Bcl-xL inhibitors A-1155463 and A-1331852 (Fig. 1a) exhibited a synergy when combined with irradiation selectively targeting HNSCC cells and ODA, but not NOF or CAF (Fig. 1b and S3). A-1155463 exhibited a synergy when combined with irradiation in 11 HNSCC cell lines, whereas A-1331852 exhibited a synergy in 10 HNSCC cell lines and navitoclax in 8 HNSCC cell lines (Fig. 1b and S3, Table S3). Additionally, p53-mutated HNSCC cell lines showed a higher synergy between BH3 mimetics and irradiation than wild-type HNSCC cell lines (Figs. S4e–g). The Bcl-xL inhibitors and navitoclax exhibited noninteractive effects on NOF and CAF when combined with irradiation

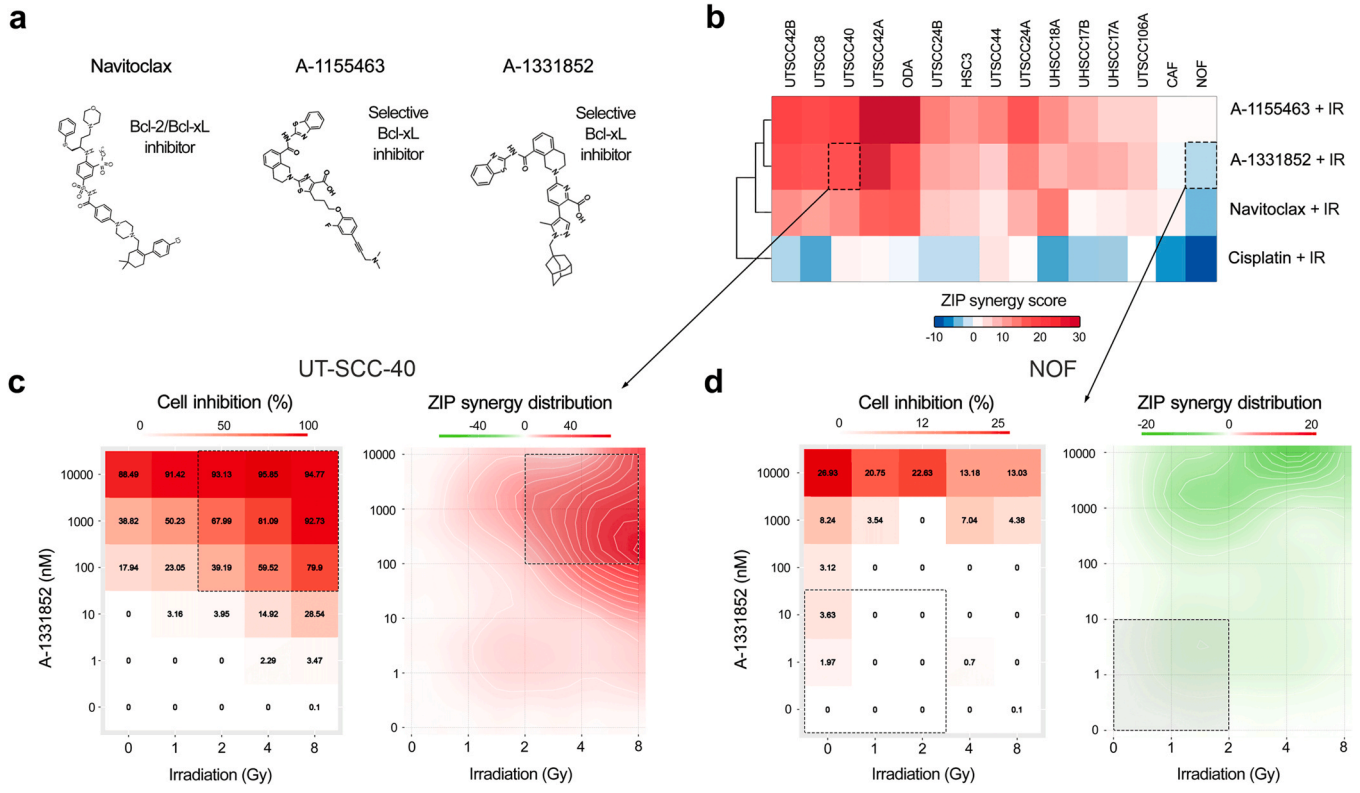

Fig. 1. The synergy validation of three BH3 mimetics tested on 12 HNSCC cell lines, CAF, NOF, and ODA grown on a Myogel matrix. (a) The BH3 mimetics used in this study. (b) HTS revealed a strong synergy between BH3 mimetics and irradiation in HNSCC and ODA cell lines, but noninteractive effects on CAF and NOF. (c) A-1331852 inhibited tongue carcinoma cell (UT-SCC-40) viability as a single agent and exhibited a strong synergy when combined with irradiation. (d) A-1331852 had a very low effect on NOF as a single agent and exhibited noninteractive effects when combined with irradiation.

(Fig. 1b and S3, Table S3). Additionally, as a single agent, the Bcl-xL inhibitors and navitoclax exhibited significantly higher effectiveness in p53 wild-type HNSCC cell lines and ODA than cell lines with mutated p53 (Figs. S4a–c). However, no similar effect was observed with cisplatin (Fig. S4d). Furthermore, the Bcl-xL inhibitors exhibited only a weak effect on NOF and CAF (Fig. 1b, 1d, and S4). Surprisingly, cisplatin exhibited noninteractive effects on all 15 tested cell lines (Fig. 1b, S3, and S4h). Overall, as a single agent, the BH3 mimetics were more effective than cisplatin (Fig. S4).

3.2. Both Bcl-xL inhibitors, A-1155463 and A-1331852, induced apoptosis in HNSCC cell lines, significantly increasing following irradiation

To study the effects of Bcl-xL inhibitors, A-1155463 and A-1331852, on HNSCC cell proliferation and apoptosis, we performed a real-time, automated apoptosis assay on two HNSCC cell lines (UT-SCC-40 and UT-SCC-42A). As expected, both Bcl-xL inhibitors acted similarly and significantly reduced UT-SCC-40 cell proliferation as a single agent in a dose-dependent manner, whereas in UT-SCC-42A, the Bcl-xL inhibitors exhibited a limited effect on cell proliferation (Fig. 2a). When combined with irradiation, the Bcl-xL inhibitors halted cell proliferation in both cell lines after two days of compound administration already at a 10-nM concentration, although the effects were more effective at higher doses (100 and 1000 nM; Fig. 2a).

Both Bcl-xL inhibitors induced immediate apoptosis in a dose-dependent manner in both cell lines; however, in UT-SCC-40 the effect was much more pronounced than in UT-SCC-42A (Fig. 2b). Furthermore, the Bcl-xL inhibitor and irradiation combinations led to a significantly higher apoptotic index compared with a monotherapy (Fig. 2b). After 72 hours, the apoptotic index in the Bcl-xL inhibitor-treated UH-SCC-40 cells appeared four to five times higher than the untreated cells (Fig. 2b). Furthermore, the Bcl-xL inhibitor–irradiation combination caused a sevenfold increase in the apoptotic index than that in the untreated cells, and the compounds with irradiation doubled the apoptotic index compared with irradiated cells leading to complete cell death (1.0; Fig. 2b). In UT-SCC-42A, the Bcl-xL inhibitors demonstrated a limited effect as a single agent (Fig. 2b). However, the Bcl-xL inhibitor–irradiation combinations led to a more than 25-fold increase in the apoptotic index compared with untreated cells and a ninefold increase compared with irradiated cells, leading to near-complete cell death (1.0; Fig. 2b).

The differences between treatment-induced apoptosis were quantified by calculating the area under the curve (AUC) for the apoptotic index (Fig. 2c). Both Bcl-xL inhibitors as single agents significantly increased the apoptotic ratio AUC compared with untreated cells at all doses except 10 nM in UT-SCC-40 (Fig. 2c). When combined with irradiation, the Bcl-xL inhibitors significantly increased the apoptotic index AUC compared with untreated and irradiated cells (Fig. 2d). Compared with the Bcl-xL inhibitors as a single agent, concomitant irradiation significantly increased the apoptotic ratio AUC for all doses (Fig. 2c).

No significant differences in the apoptotic ratio AUC were observed between the untreated and the irradiated cells in both cell lines (Fig. 2c). Overall, the UT-SCC-40 cells were more sensitive to irradiation than the UT-SCC-42A cells. Irradiation decreased cell proliferation and induced apoptosis in UT-SCC-40, whereas the UT-SCC-42A cell line was more resistant to radiation. Irradiation had no effect on the UT-SCC-42A cell proliferation and only slightly increased apoptosis compared with the control (Fig. 2).

3.3. Combination of A-1331852/navitoclax and irradiation decreased clonogenicity compared to untreated HNSCC cells and monotherapies

Clonogenic survival assay revealed that the UT-SCC40 cell line exposed to A-1331852 significantly decreased clonogenicity compared with untreated cells and the A-1331852–irradiation combination compared with irradiated cells at all concentrations (Fig. 3a). Compared with untreated cells, the A-1331852–irradiation combination decreased the clonogenicity of both cell lines (UT-SCC40 and UT-SCC-42A) at all concentrations. The navitoclax–irradiation combination at all concentrations significantly decreased the clonogenicity of both cell lines

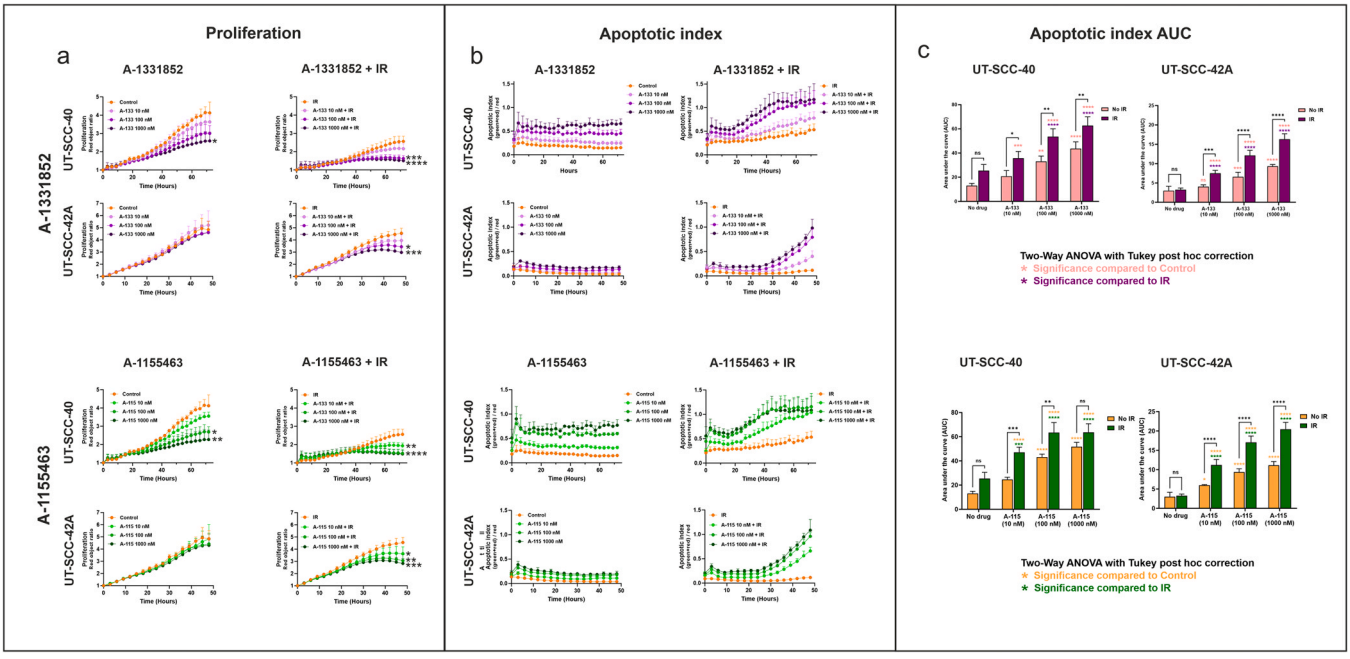

Fig. 2. The combination of both Bcl-xL inhibitors and irradiation halt proliferation and trigger apoptosis in HNSCC cells. (a) Effects of A-1331852 (A-133) and A-1155463 (A-115) on the proliferation of two cell lines as a single agent and when combined with irradiation (IR: 8 Gy). Statistical differences were determined using a one-way ANOVA with the Tukey post-hoc correction. (b) The Bcl-xL inhibitors increased the apoptotic index as a single agent and in combination with irradiation. (c) Differences between treatments induced apoptosis quantified by calculating the AUC for the apoptotic index. Data are presented as mean ± standard deviation (SD) between experiments (n = 4). Asterisks indicate a significant effect of treatment compared with the control and IR. *$p < 0.05$, **$p \leq 0.01$, ***$p \leq 0.001$, **** $p \leq 0.0001$.

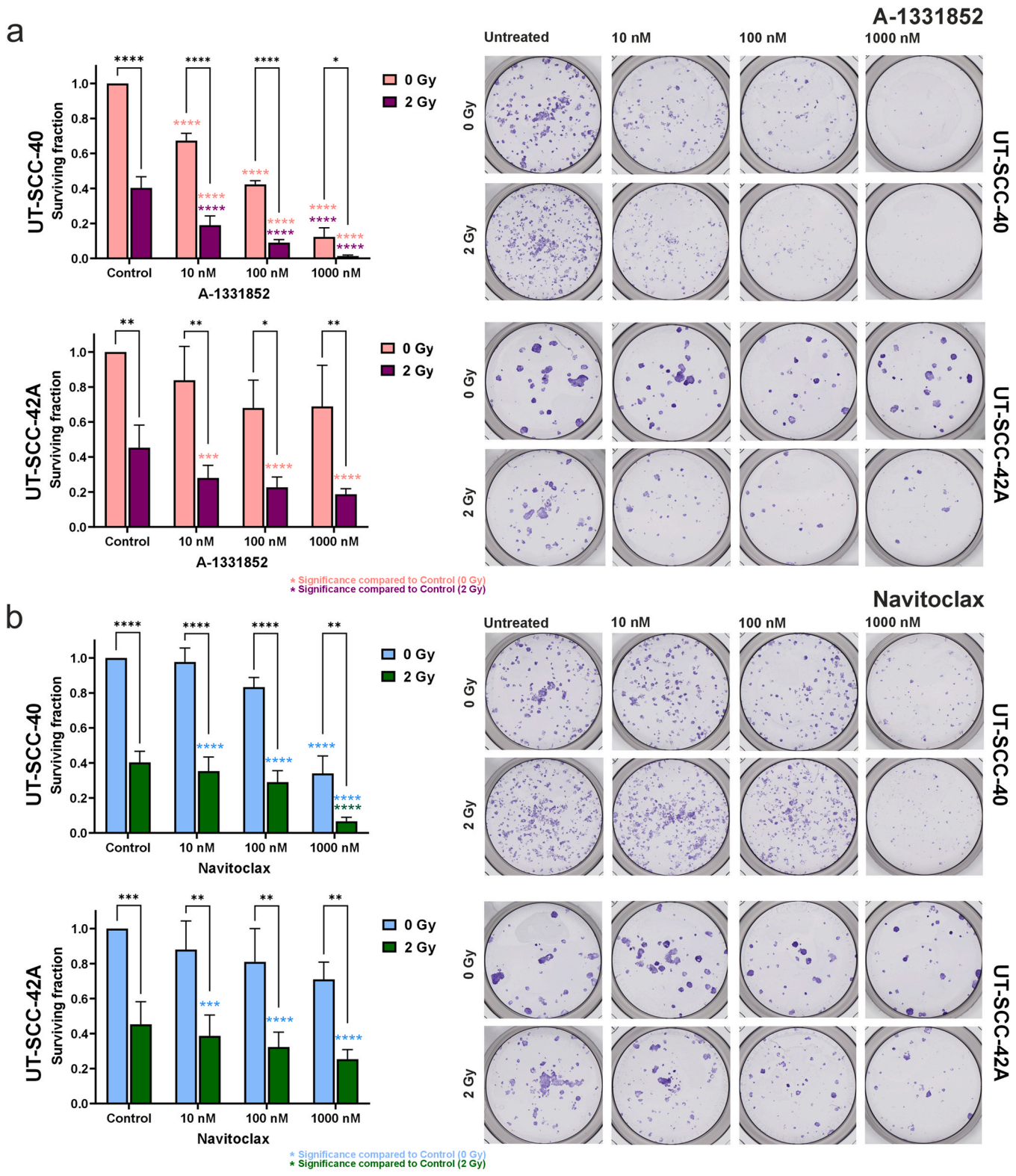

Fig. 3. Clonogenic viability of HNSCC cells after treatment with A-1331852 or navitoclax as a single agent and combined with irradiation. (a) The UT-SCC40 cell line exposed to the A-1331852–irradiation combination significantly decreased clonogenicity compared with untreated cells and monotherapies, already at a 10-nM concentration. Additionally, monotherapy significantly decreased the UT-SCC-40 cell clonogenicity compared with untreated cells. The A-1331852–irradiation combination decreased the clonogenicity of both cell lines compared with untreated cells. (b) The navitoclax–irradiation combination significantly decreased the clonogenicity of both cell lines compared with the untreated cells and also irradiated cells at a 1000-nM concentration in UT-SCC-40. The clonogenic viability was presented as the surviving fraction relative to untreated, nonirradiated cells. Data are presented as the standard deviation (SD) between experiments (n = 3). *$p <$ 0.05, **$p \leq 0.01$, ***$p \leq 0.001$, ****$p \leq 0.0001$.

compared with the untreated cells and also with irradiated cells at a 1000-mM concentration in UT-SCC-40 (Fig. 3b). Compared with single agent treatments, concomitant irradiation significantly decreased the clonogenicity for all doses (Fig. 3).

3.4. A-1331852 significantly reduced HNSCC cell invasion length and area in the spheroid assay

To further study the effects of BH3 mimetics on HNSCC, we performed a spheroid invasion assay applying three doses of BH3 mimetics and irradiation (8 Gy) using the UT-SCC-42A cells. Overall, irradiation had only a modest effect on the UT-SCC-42A cell invasion when compared with untreated cells (Fig. 4). Moreover, irradiation had no impact on the invasion length (Fig. 4b), but a fractionally reduced invasion area compared with the control, although the difference was not statistically significant (Fig. 4c). All three doses of A-1331852 effectively reduced the invasion length and area as a single agent, and the effect was enhanced when combined with irradiation (Fig. 4a). However, due to the wide standard deviation, only the 1000-nM dose resulted in statistically significant differences on day three for both the invasion length and area (Fig. 4bc). For the invasion areas, the 100-nM dose combined with irradiation resulted in statistically different results compared with the control group (Fig. 4c).

3.5. A-1155463 exhibited a decreasing trend for HNSCC cell invasion, whereas navitoclax had no effect on cell invasion in a spheroid assay

A-1155463 reduced the UT-SCC-42A cell invasion length and area dose-dependently, although it lacked statistical significance due to the large variation between experiments (Fig. 5). The A-1155463–irradiation combination marginally reduced the invasion area (Fig. 5c), but not the invasion length (Fig. 5b). Surprisingly, navitoclax did not impact the UT-SCC-42A cell invasion length or area (Fig. 6).

3.6. A-1331852 and navitoclax significantly reduced the tumor area and metastasis in zebrafish larvae

To validate the effects of BH3 mimetics on the HNSCC tumor area and metastasis *in vivo*, we employed a zebrafish larvae xenograft model. Since BH3 mimetics have previously been administrated in zebrafish larvae with minimal toxicity [7], we performed cytotoxicity tests for BH3 mimetics as a single agent and together with irradiation using zebrafish.

The analysis revealed that irradiation alone had no effect on the tumor area in the fish (Fig. 7b). As a single agent, navitoclax significantly reduced the UT-SCC-42A tumor area, while the navitoclax–irradiation combination lacked such an effect (Fig. 7b). A-1331852 as a single agent and when combined with irradiation significantly reduced the tumor area compared with the control group (Fig. 7b). In total, 31% [95% confidence interval (CI) 25.5–43.2%] of the control fish and 31% (95% CI 19.9–42.5%) of the irradiated fish developed metastases (Fig. 7c). Furthermore, 18.8% (95% CI 10.4–28.4%) of the fish treated with navitoclax developed metastasis; however, the differences when compared with controls were not statistically significant. Fish treated with the navitoclax–irradiation combination had significantly less metastases compared with the control group (16.9%; 95% CI 8.2–25.0%; Fig. 7c). A-1331852 as a single agent and when combined with irradiation emerged as the most effective treatment to reduce metastases, given that these treatments reduced metastases to 3.4% (95% CI 1.0–11.7%) and 3.4% (95% CI 1.0–11.7%), respectively.

4. Discussion

The Bcl-xL protein is commonly upregulated in HNSCC [5] and a high Bcl-xL expression in the HNSCC tumor area has reportedly correlated with the presence of lymph node metastases and lower survival rates [8,9]. However, only a few Bcl-xL inhibitor *in vitro* studies for HNSCC exist and, in March 2023, no records of ongoing clinical trials investigating the effects of any BH3 mimetic drugs on HNSCC were found. The high-throughput screen of a large compound library was previously performed, which identified the potential efficacy of navitoclax, a Bcl-2- and Bcl-xL-inhibiting BH3 mimetic, in HNSCC in combination with irradiation [12]. In the same study, the Bcl-2 inhibitor venetoclax (ABT-199) and Bcl-2/Mcl-1 inhibitor AT-101 (gossypol) displayed only a modest efficacy and lacked synergistic effects when combined with irradiation. In line with these findings, Carter *et al.* previously reported that venetoclax and the Mcl-1 inhibitor S63845 failed to induce apoptosis in six HNSCC cell lines [7]. Therefore, we concluded that the efficacy and synergistic properties with irradiation rely on the inhibition of Bcl-xL or the dual inhibitor of Bcl-2 and Bcl-xL. Our aim here was to investigate the effects of novel selective Bcl-xL inhibitors simultaneously with the previously *in vitro*–tested navitoclax. To achieve this, we performed a viability-detecting HTS to investigate the possible anticancer effects and synergy with irradiation using novel compounds targeting only the Bcl-xL protein (A-1155463 and A-1331852) [26]. Our results indicate that the novel Bcl-xL-selective inhibitors, A-1155463 and A-1331852, exhibit selective anticancer effects and a strong synergy with irradiation similar to simultaneously and previously tested navitoclax (Fig. 1) [12]. In contrast to HNSCC cell lines, in normal oral and cancer-associated fibroblasts, the combination of BH3 mimetics and irradiation exhibited predominantly noninteractive responses. Furthermore, as a single agent, all three BH3 mimetics had only a minor inhibitory effect on the viability of fibroblasts (Fig. 1). Interestingly, HPV-transfected dysplastic keratinocytes were highly sensitive to all compounds applied in HTS, including cisplatin; moreover, BH3 mimetics acted synergistically with irradiation. These results indicate that BH3 mimetics can selectively target HPV-infected epithelial cells. However, this hypothesis warrants further investigation. Surprisingly, the reference chemotherapeutic agent cisplatin exhibited only additional or antagonistic effects when combined with irradiation on HNSCC cell lines. Furthermore, BH3 mimetics appeared superior in effectiveness compared with cisplatin. Based on this finding, it is possible that BH3 mimetics could replace cisplatin in chemoradiotherapy in patients unable to tolerate the severe adverse effects of cisplatin.

The most frequent genomic alteration in HNSCC is an inactivating mutation of p53, accounting for 60–80% of HNSCC cases [27]. One previous study showed that navitoclax synergizes with radiotherapy regardless of the p53 mutation status [28]. In our study, a majority of the HNSCC cell lines showed strong synergism between radiation. However, p53-mutant HNSCC cell lines showed a higher synergy between BH3 mimetics and irradiation than wild-type HNSCC cell lines (Figs. S4e–h). Furthermore, as a single agent, the Bcl-xL inhibitors and navitoclax exhibited significantly higher effectiveness in p53 wild-type HNSCC cell lines than in cell lines with mutated p53 (Fig. S4).

In line with a previous report on navitoclax [12], our apoptosis assay revealed that both Bcl-xL inhibitors, A-1155463 and A-1331852, significantly induced apoptosis in a dose-dependent manner and halted cell proliferation when combined with irradiation in both HNSCC cell lines tested (Fig. 2). As a single agent, both Bcl-xL inhibitors reduced UT-SCC-40 cell proliferation and induced apoptosis in a dose-dependent manner. In contrast to our findings, Carter *et al.* previously found that A-1331852 failed to induce pronounced apoptosis *in vitro* in six HNSCC cell lines [7]. However, apoptosis was measured using a different method, phosphatidylserine (PS) externalization, and only a 100-nM dose was applied [7]. The authors reported that the combination of the BH3 mimetics, A1331852, and Mcl-1 inhibitor S63845, induced apoptosis in all six HNSCC cell lines. A recent report of another selective Bcl-xL inhibitor WEHI-539, at a dose of 750–5000 nM, demonstrated synergistic effects with fractionated radiation on three HNSCC cell lines through the FACS analysis of cell death [29]. The authors concluded that Bcl-xL inhibition plays an important role in radiosensitizing HNSCC cells

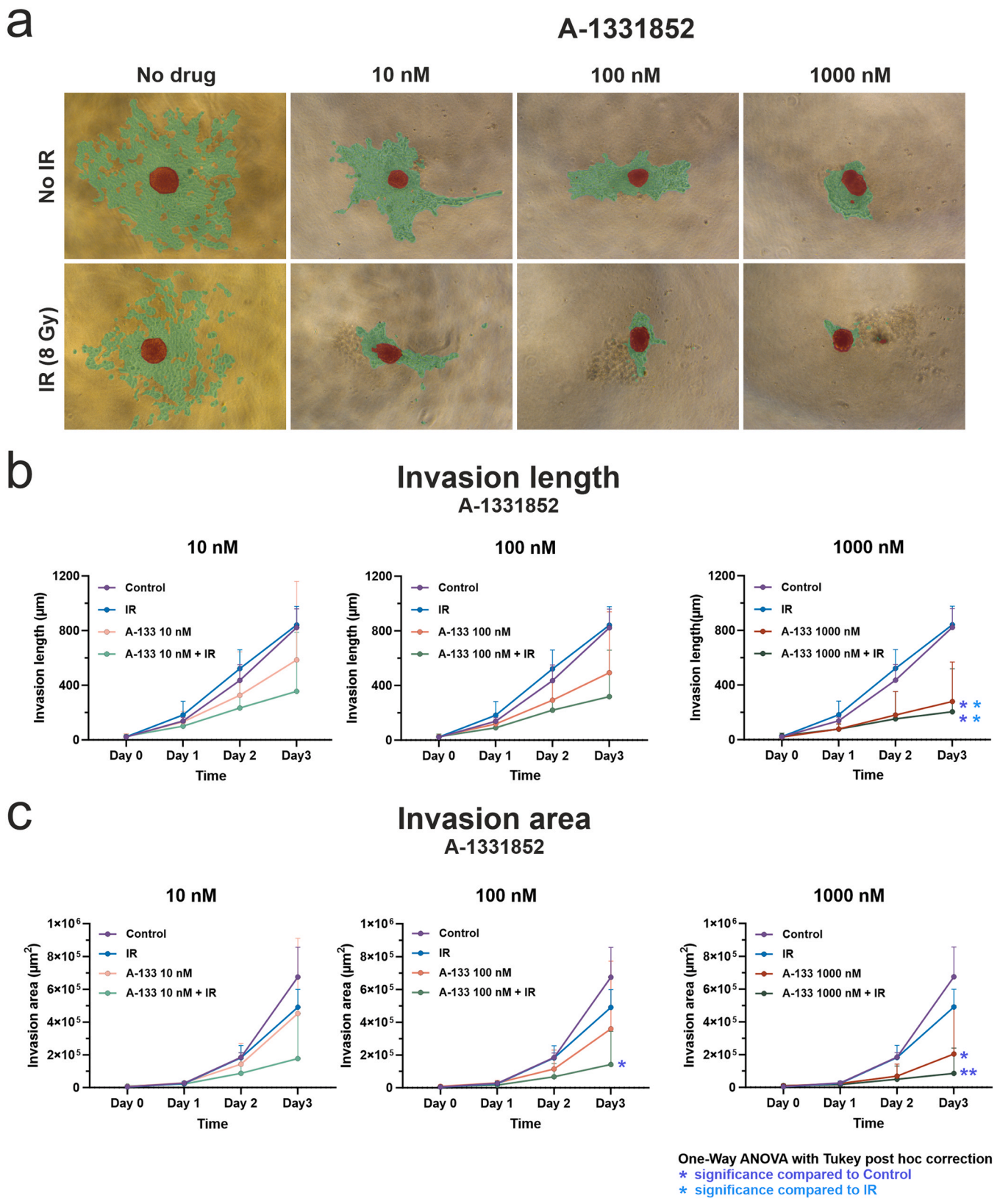

Fig. 4. The effects of A-1331852 (A-133) and irradiation on laryngeal carcinoma (UT-SCC-42A) cell invasion. (a) Representative images of the spheroid invasion with different treatment combinations on the third day (day 3). (b) The UT-SCC-42A invasion length and (c) area over three days when treated with three doses of A-1331852 as a single agent or in combination with irradiation. Statistical differences were determined using a one-way ANOVA with the Tukey post-hoc correction. Data are presented as mean ± standard deviation (SD) between experiments (n = 4). *$p \leq 0.05$, **$p \leq 0.01$.

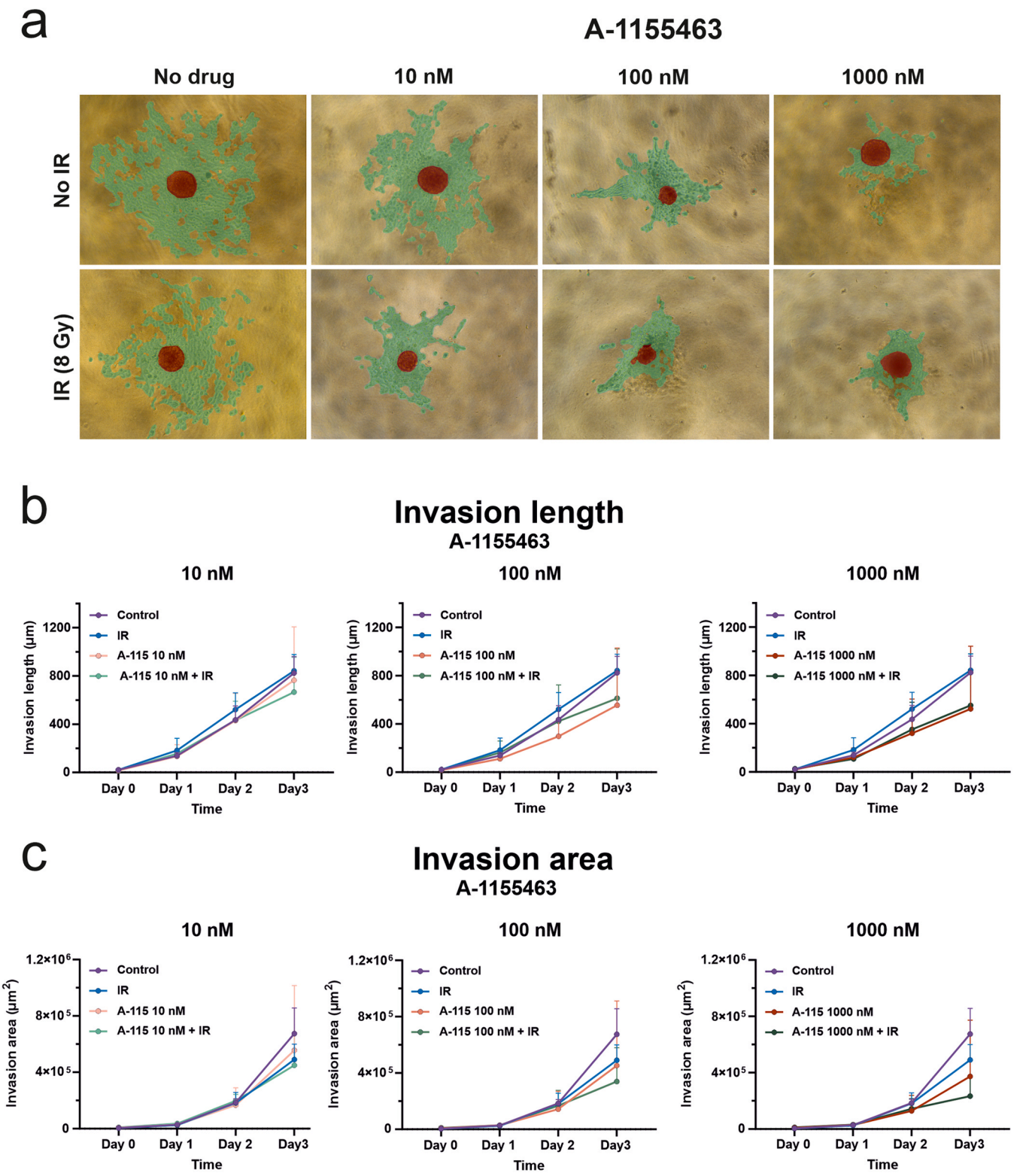

Fig. 5. The effects of A-1155463 (A-115) and irradiation on the UT-SCC-42A cell invasion. (a) Representative images of the spheroid invasion with different treatment combinations on the third day. (b) The UT-SCC-42A invasion length and (c) area were measured over three days when treated with A-1155463 as a single agent or in combination with irradiation.

[29]. However, WEHI-539 is predeceased and a less likely version of A-1155463, possessing a possibly toxic moiety and poor oral solubility [30].

In the clonogenic survival assay, A-1331852 emerged as more effective than navitoclax and the UT-SCC-40 cell line was more sensitive to both compounds as a single agent and in combination with radiotherapy (Fig. 3). Both of the tested BH3 mimetics exhibited significant synergistic effects on the clonogenicity of UT-SCC-40 cells, while the results for the UT-SCC-42A cells were less convincing. In UT-SCC-40 cells, A-1331852 significantly decreased the clonogenicity as a single

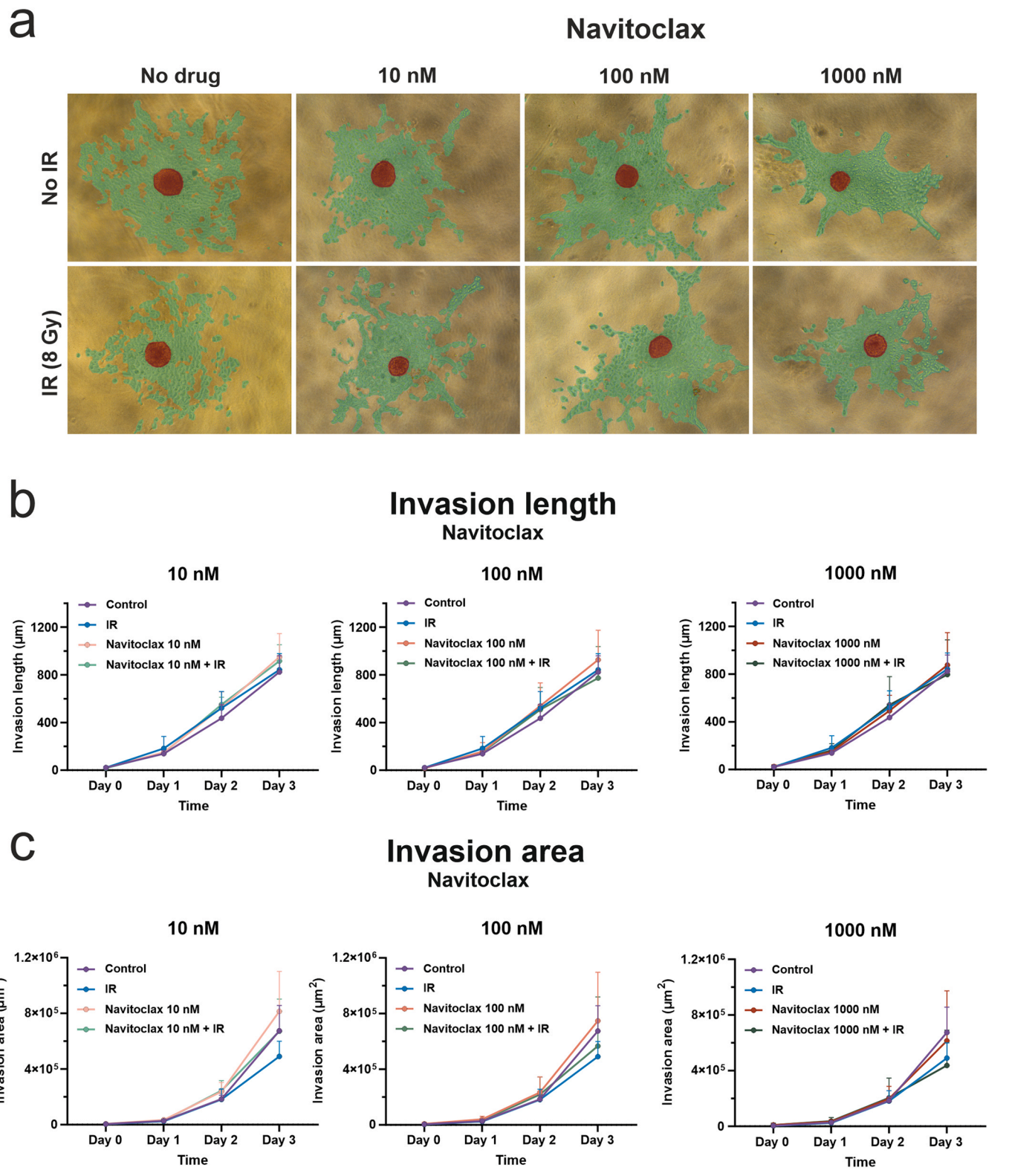

Fig. 6. The effects of navitoclax and irradiation on the UT-SCC-42A cell invasion. (a) Representative images of the spheroid invasion with different treatment combinations on the third day. (b) The UT-SCC-42A invasion length and (c) area over three days when treated with navitoclax as a single agent or in combination with irradiation.

agent compared with untreated cells already at 10-mM concentrations, whereas for navitoclax clonogenicity decreased only at 1000-nM concentrations. Carter *et al.* reported a similar synergism between A-1331852 (100 nM) and irradiation (2 Gy), however, only in one of six HNSCC cell lines [7].

A high Bcl-xL expression in the tumor area has reportedly correlated with the presence of lymph node metastases in HNSCC [8,9]. Furthermore, the Bcl-xL overexpression increases *in vitro* cell invasion in many cancer types such as melanoma and colorectal and breast cancers [31–33]. However, no *in vitro* studies have shown that the

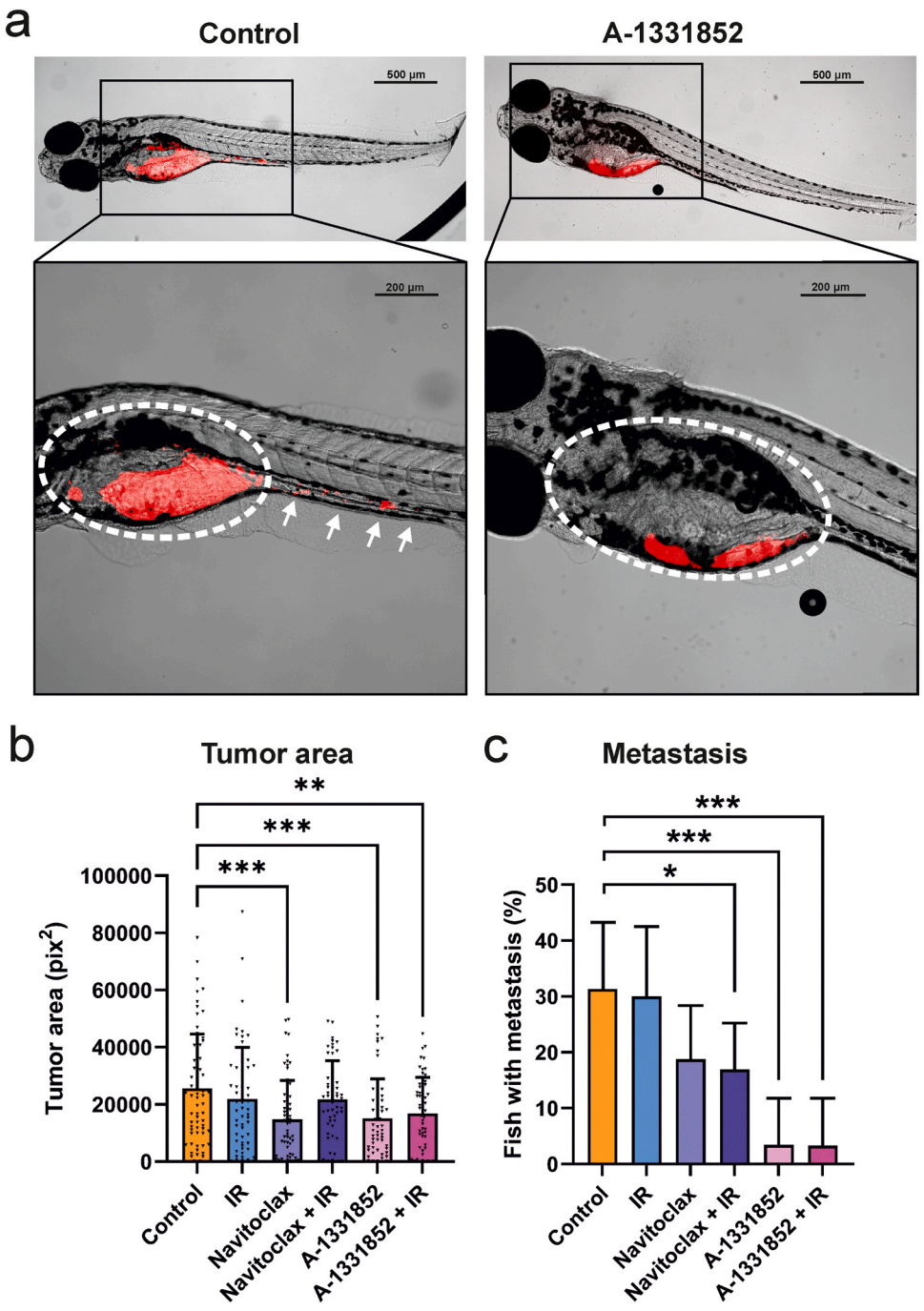

Fig. 7. The effects of A-1331852 and navitoclax and irradiation on the tumor area and metastasis in the zebrafish xenograft (a) Reduction to the tumor area and metastasis in the zebrafish larvae following A-1331852 treatment. (b) Navitoclax (1000 nM) and A-1331852 (1000 nM) as a single agent and when combined with irradiation (8 Gy) significantly reduced the tumor area. Statistical differences were determined using a one-way ANOVA with the Bonferroni correction. (c) The navitoclax–irradiation combination significantly decreased the percentage of fish with metastasis (18.8%) compared with the control group (31%), while A1331852 as a single agent and combined with irradiation emerged as the most effective treatment, reducing metastases to 3.4%. The Wald Z-test was used to identify significant differences. Data are presented as the mean ± standard deviation (SD) between individual fish (n = 58–67). $^{*}p < 0.05$, $^{**}p \leq 0.01$, $^{***}p \leq 0.001$.

overexpression or inhibition of Bcl-xL interferes with HNSCC cell invasion. For the first time to our knowledge, we demonstrated that Bcl-xL inhibition reduces HNSCC cell invasion *in vitro* using the spheroid invasion model (Fig. 4). Specifically, our data revealed that A-1331852 significantly reduced the invasion length and area of the radiation-resistant HNSCC cell line (UT-SCC-42A) at a 1000-nM dose as a single agent and simultaneously when combined with irradiation even at a 100-nM dose (Fig. 4). The other selective Bcl-xL inhibitor A-1155463 exhibited a trend towards reducing HNSCC invasion, although the differences lacked statistical significance due to the large variation between experiments (Fig. 5). The difference in efficacy among Bcl-xL inhibitors may be due to the fact that A-1331852 is a re-engineered version of A-1155463 and, thus, remains more stable in three-dimensional (3D) cell culture conditions [26]. Surprisingly, navitoclax did not reduce the HNSCC cell invasion area or length (Fig. 6). By contrast, A-1331852 reportedly has a higher binding affinity to Bcl-xL (Ki < 0.01 nM) than navitoclax (Ki < 1 Nm) [34,35]. Our results suggest that Bcl-xL may play a greater role in HNSCC cell invasion than

Bcl-2.

Mice have long been considered the gold standard for xenografts. However, the mouse xenograft has consistently failed to predict the human response to anticancer compounds in clinical trials [36]. According to new legislation from the US Food and Drug Administration (FDA), new medicines no longer require animal tests before human clinical trials [37]. The zebrafish xenograft has become a widely applied model in cancer research, and is a frequently used model for the *in vivo* validation of anticancer drug efficacy [36]. Our zebrafish assays revealed that A-1331852 as a single agent and when combined with irradiation significantly reduced the tumor area and inhibited metastasis in zebrafish larvae at 5 dpf (Fig. 7). To our knowledge, this is the first *in vivo* report of A-1331852 and the A-1331852–irradiation combination assessing HNSCC tumor area and metastasis. A previous study reported that the combination of A-1331852 and S63845 at 1000–2000 nM doses reduced the HNSCC tumor burden in zebrafish at 5 dpf [7]. However, the authors did not report the effect of A-1331852 in zebrafish as a single agent. Navitoclax has never been assessed in the HNSCC zebrafish xenograft. However, navitoclax exhibited a significant reduction in oral cancer cell growth in a nude mice xenograft [38]. In line with that report, we demonstrated that navitoclax significantly reduced the HNSCC tumor cell area *in vivo* (Fig. 7). Additionally, the combination of navitoclax and irradiation significantly reduced metastasis in zebrafish larvae. Interestingly, in contrast to the two-dimensional (2D) *in vitro* assays, in a 3D spheroid and in zebrafish, irradiation appeared ineffective and failed to significantly increase the drug effect.

Cancer cells are known to be more chemo- and radioresistant in more complex models, as in 3D and *in vivo* assays compared with traditional 2D cell assays [39,40]. Cells cultured in 3D have displayed different responses to drugs than cells cultured in 2D for several reasons: differences in physical and physiological properties, the organization of surface receptors, differences in cell cycle stages, and differences in local pH levels within the cells [39,40]. Furthermore, the extracellular matrices (ECM) used as scaffolds in 3D models may affect drug responses due to the presence of ECM components such as matrix proteins, glycosaminoglycans, and growth factors [39]. Zebrafish avatars are reportedly promising tools for personalized medicine since they can predict patient treatment response and radioresistant clones with a high accuracy [41,42]. HNSCC patient cells have been tested in *in vitro* and in zebrafish larvae xenograft and compared with each other and with patients' clinical responses [41]. This study reports resistance in radiation and chemoradiation with some of the HNSCC patient cells tested in zebrafish larvae compared with *in vitro* cultures [41]. Interestingly, in this study, the zebrafish assay emerged as the most promising tool for predicting an HNSCC patient's clinical response, with a 77% accuracy [41]. The abovementioned factors may play a role in the radioresistance of cancer cells in our spheroid and zebrafish assays.

All three BH3 mimetic–irradiation combinations demonstrated synergism in cell viability as well as in apoptosis and clonogenicity in 2D cell assays, however, in the spheroid assay, only A-133152 as a single agent and when combined with irradiation had a significant effect on cell invasion. Furthermore, the zebrafish assay findings differed from the 2D *in vitro* results since irradiation failed to enhance the drug's effects. In fish, the A-1331852–irradiation combination turned out to be an equally effective treatment for reducing the tumor area as a monotherapy, and both treatments equally prevented the occurrence of metastases. The addition of radiation therapy to navitoclax treatment did not significantly reduce the size of the cancer, but it did reduce metastases slightly more effectively than when used as a single agent. In summary, based on our *in vivo* findings, it remains unclear whether combination therapy is a more effective option than monotherapy. Therefore, further preclinical evaluation is needed to confirm these findings before clinical application.

As demonstrated in navitoclax-treated patients, Bcl-xL inhibition may cause adverse effects such as thrombocytopenia [43]. A-1331852 reportedly reversibly reduces circulating platelets in rats similar to navitoclax [34]. However, this may not prohibit the use of Bcl-xL inhibitors in the context of head and neck cancers, since similar adverse effects are frequently tolerated in regular chemotherapy regimens. A recent clinical trial demonstrated that navitoclax combined with ruxolitinib was well-tolerated in patients with myelofibrosis, supporting the feasibility of Bcl-xL inhibition in patients, although thrombocytopenia was noted as the most frequent side effect [44]. Platelet transfusion or a platelet-sparing Bcl-xL drug, such as a proteolysis-targeting chimera (PROTAC) [45], could circumvent the potential adverse effects on normal thrombopoiesis.

5. Conclusions

Taken together, our comprehensive *in vitro* assays revealed that novel BH3 mimetics (A-1331853, A-1155463, and navitoclax) and irradiation possess synergistic anticancer effects on HNSCC cell viability, proliferation, clonogenicity, and apoptosis. In HTS, BH3 mimetics decreased viability in p53 wild-type HNSCC cell lines more efficiently than in p53-mutant cell lines. Furthermore, BH3 mimetics selectively targeted HNSCC and dysplastic keratinocytes, but not fibroblasts. As one of the most promising findings—and, to our knowledge, the first such report—we demonstrated that the Bcl-xL inhibitor A-1331852 significantly reduced invasion *in vitro* and metastasis *in vivo*. Furthermore, here we report for the first time that A-1331852 and navitoclax significantly reduced the tumor area in zebrafish larvae. In conclusion, given the poor prognosis associated with head and neck cancers and the limited targeted therapy options, we propose Bcl-xL as a promising target for further exploration. Our results, thus, encourage further preclinical investigation of BH3 mimetics, especially A-1331852, as a single agent or combined with irradiation as a treatment for HNSCC.

Funding

This project was funded by the Cancer Foundation Finland, the Sigrid Juselius Foundation, the Jane and Aatos Erkko Foundation, the Otto A. Malm Foundation, the Minerva Foundation's Selma and Maja-Lisa Selander's Fund, and the Helsinki University Central Hospital research funds.

CRediT authorship contribution statement

Ahmed Al-Samadi: Writing – review & editing, Supervision, Conceptualization. **Ilya Belevich:** Writing – review & editing, Software, Methodology. **Tuula Salo:** Writing – review & editing, Supervision, Resources, Conceptualization. **Laura Turunen:** Writing – review & editing, Methodology, Conceptualization. **Bruno Cavalcante:** Writing – review & editing, Methodology, Investigation. **Filipp Ianevski:** Writing – review & editing, Visualization, Formal analysis, Data curation. **Katja Korelin:** Writing – review & editing, Writing – original draft, Visualization, Software, Project administration, Methodology, Investigation, Formal analysis, Conceptualization. **Wafa Wahbi:** Writing – review & editing, Methodology, Formal analysis. **Mayke Oostveen:** Writing – review & editing, Software, Methodology, Formal analysis, Data curation.

Declaration of Competing Interest

The authors declare that they have no known competing financial interests or personal relationships that could have appeared to influence the work reported in this paper.

Data availability

Data will be made available on request.

Acknowledgements

We thank the DDCB core facility (FIMM High-Throughput Biomedicine Unit), supported by the University of Helsinki and Biocenter Finland, for their technical support. Special thanks are extended to Katja Suomi, Swapnil Potdar, and Jani Saarela for their technical support. The authors acknowledge the assistance and support of Harri Jäälinoja from the Light Microscopy Unit, Institute of Biotechnology, for assisting with the image analysis. The Institute of Biotechnology (IB) and the Electron Microscopy Unit (EMBI) were supported by Biocenter Finland and the Helsinki Institute of Life Science. We acknowledge the Biomedicum Imaging Unit (University of Helsinki, Helsinki, Finland) for their technical support with microscopy imaging. We thank Meri Sieviläinen for image analysis support, Susannah von Hofsten for her technical assistance with the HTS pilot experiment, and Aleksandr Ianevski for his assistance with SynergyFinder software. We also thank Maija Risteli, Sarianna Tuovinen, Natalie Fernandes, and Arina Värä for their assistance with clonogenic survival assays. Finally, the authors thank the Biostatistics Unit (University of Helsinki, Helsinki, Finland) for assistance with statistical analysis.

Appendix A. Supporting information

Supplementary data associated with this article can be found in the online version at doi:10.1016/j.biopha.2024.116719.

References

[1] H. Sung, J. Ferlay, R.L. Siegel, M. Laversanne, I. Soerjomataram, A. Jemal, F. Bray, Global Cancer Statistics 2020: GLOBOCAN estimates of incidence and mortality worldwide for 36 cancers in 185 countries, CA Cancer J. Clin. 71 (2021) 209–249.
[2] R.L. Siegel, K.D. Miller, A. Jemal, Cancer statistics, 2017, CA Cancer J. Clin. 67 (2017) 7–30.
[3] J. Sia, R. Szmyd, E. Hau, H.E. Gee, Molecular mechanisms of radiation-induced cancer cell death: a primer, Front Cell Dev. Biol. (2020), https://doi.org/10.3389/FCELL.2020.00041.
[4] J. Kale, E.J. Osterlund, D.W. Andrews, BCL-2 family proteins: changing partners in the dance towards death, Cell Death Differ. 2018 25 125 (2017) 65–80.
[5] G. Melo, C.A.B. Silva, A. Hague, E.K. Parkinson, E.R.C. Rivero, Anticancer effects of putative and validated BH3-mimetic drugs in head and neck squamous cell carcinomas: An overview of current knowledge, Oral. Oncol. 132 (2022) 105979.
[6] J.C. Pena, C.B. Thompson, W. Recant, E.E. Vokes, C.M. Rudin, 1999, , Bcl-x L and Bcl-2 Expression in Squamous Cell Carcinoma of the Head and Neck10.1002/(SICI)1097-0142(19990101)85:1.
[7] R.J. Carter, M. Milani, M. Butterworth, et al., Exploring the potential of BH3 mimetic therapy in squamous cell carcinoma of the head and neck, Cell Death Dis. 2019 10 12 (10) (2019) 1–10.
[8] H. Ziai, A. Alenazi, M. Hearn, D.A. O'Connell, L. Puttagunta, B. Barber, J.R. Harris, H. Seikaly, V.L. Biron, The association of Bcl-xL and p53 expression with survival outcomes in oropharyngeal cancer, Cancer Biomark. 24 (2019) 141–151.
[9] K. Zhang, K. Jiao, Z. Xing, L. Zhang, J. Yang, X. Xie, L. Yang, Bcl-xL overexpression and its association with the progress of tongue carcinoma, Int J. Clin. Exp. Pathol. 7 (2014) 7360.
[10] FDA approves venetoclax for CLL and SLL | FDA. ⟨https://www.fda.gov/drugs/resources-information-approved-drugs/fda-approves-venetoclax-cll-and-sll⟩. Accessed 6 Jun 2023.
[11] N.N. Mohamad Anuar, N.S. Nor Hisam, S.L. Liew, A. Ugusman, Clinical review: navitoclax as a pro-apoptotic and anti-fibrotic agent, Front Pharm. 11 (2020) 1817.
[12] K. Tuomainen, A. Hyytiäinen, A. Al-Samadi, et al., High-throughput compound screening identifies navitoclax combined with irradiation as a candidate therapy for HPV-negative head and neck squamous cell carcinoma, Sci. Rep. (2021), https://doi.org/10.1038/s41598-021-94259-5.
[13] F. Ahmadinejad, T. Bos, B. Hu, E. Britt, J. Koblinski, A.J. Souers, J.D. Leverson, A. C. Faber, D.A. Gewirtz, H. Harada, Senolytic-mediated elimination of head and neck tumor cells induced into senescence by cisplatin, Mol. Pharm. 101 (2022) 168–180.
[14] D. Oda, L. Bigler, P. Lee, R. Blanton, HPV immortalization of human oral epithelial cells: a model for carcinogenesis, Exp. Cell Res 226 (1996) 164–169.
[15] L.M. Sobral, K.G. Zecchin, S.N. De Aquino, M.A. Lopes, E. Graner, R.D. Coletta, Isolation and characterization of myofibroblast cell lines from oral squamous cell carcinoma, Oncol. Rep. 25 (2011) 1013–1020.
[16] M. Vered, D. Dayan, R. Yahalom, A. Dobriyan, I. Barshack, I.O. Bello, S. Kantola, T. Salo, Cancer-associated fibroblasts and epithelial-mesenchymal transition in metastatic oral tongue squamous cell carcinoma, Int J. Cancer 127 (2010) 1356–1362.
[17] T. Pemovska, M. Kontro, B. Yadav, et al., Individualized systems medicine strategy to tailor treatments for patients with chemorefractory acute myeloid leukemia, Cancer Discov. 3 (2013) 1416–1429.
[18] T. Salo, M.R. Dourado, E. Sundquist, E.H. Apu, I. Alahuhta, K. Tuomainen, J. Vasara, A. Al-Samadi, Organotypic three-dimensional assays based on human leiomyoma–derived matrices, Philos. Trans. R. Soc. B Biol. Sci. (2018), https://doi.org/10.1098/rstb.2016.0482.
[19] K. Tuomainen, A. Al-Samadi, S. Potdar, et al., Human tumor–derived matrix improves the predictability of head and neck cancer drug testing, Cancers (Basel) (2020), https://doi.org/10.3390/cancers12010092.
[20] S. Potdar, A. Ianevski, J.P. Mpindi, et al., Breeze: an integrated quality control and data analysis application for high-throughput drug screening, Bioinformatics 36 (2020) 3602–3604.
[21] A. Ianevski, A.K. Giri, T. Aittokallio, SynergyFinder 3.0: an interactive analysis and consensus interpretation of multi-drug synergies across multiple samples, Nucleic Acids Res 50 (2022) W739.
[22] E. Naakka, K. Tuomainen, H. Wistrand, M. Palkama, I. Suleymanova, A. Al-Samadi, T. Salo, Fully human tumor-based matrix in three-dimensional spheroid invasion assay, J. Vis. Exp. (2019), https://doi.org/10.3791/59567.
[23] I. Belevich, M. Joensuu, D. Kumar, H. Vihinen, E. Jokitalo, Microscopy image browser: a platform for segmentation and analysis of multidimensional datasets, PLoS Biol. 14 (2016) e1002340.
[24] K. He, X. Zhang, S. Ren, J. Sun, 2016, , Deep Residual Learning for Image Recognition10.1109/CVPR.2016.90.
[25] I. Belevich, E. Jokitalo, DeepMIB: user-friendly and open-source software for training of deep learning network for biological image segmentation, PLoS Comput. Biol. 17 (2021) e1008374.
[26] L. Wang, G.A. Doherty, A.S. Judd, et al., Discovery of A-1331852, a first-in-class, potent, and orally-bioavailable BCL-XL inhibitor, ACS Med Chem. Lett. 11 (2020) 1829–1836.
[27] C.R. Leemans, Braakhuis BJM, R.H. Brakenhoff, The molecular biology of head and neck cancer, Nat. Rev. Cancer 2011 11 1 (11) (2010) 9–22.
[28] K. Tuomainen, A. Hyytiäinen, A. Al-Samadi, et al., High-throughput compound screening identifies navitoclax combined with irradiation as a candidate therapy for HPV-negative head and neck squamous cell carcinoma, Sci. Rep. 2021 11 1 (11) (2021) 1–10.
[29] B. Sobol, O. Azzam Nieto, E.L. Eberlein, et al., Specific targeting of antiapoptotic Bcl-2 proteins as a radiosensitizing approach in solid tumors, Int J. Mol. Sci. (2022), https://doi.org/10.3390/IJMS23147850.
[30] Z.-F. Tao, L. Hasvold, L. Wang, et al., Discovery of a Potent and Selective BCL-X L inhibitor with in vivo activity, ACS Med Chem. Lett. 5 (2014) 29.
[31] S. Choi, Z. Chen, L.H. Tang, Y. Fang, S.J. Shin, N.C. Panarelli, Y.T. Chen, Y. Li, X. Jiang, Y.C.N. Du, Bcl-xL promotes metastasis independent of its anti-apoptotic activity, Nat. Commun. 2016 7 1 (7) (2016) 1–13.
[32] D. Trisciuoglio, M.G. Tupone, M. Desideri, M. Di Martile, C. Gabellini, S. Buglioni, M. Pallocca, G. Alessandrini, S. D'aguanno, D. Del Bufalo, BCL-XL overexpression promotes tumor progression-associated properties, Cell Death Dis. (2017), https://doi.org/10.1038/S41419-017-0055-Y.
[33] B.C. Koehler, A.L. Scherr, S. Lorenz, T. Urbanik, N. Kautz, C. Elssner, S. Welte, J. L. Bermejo, D. Jäger, H. Schulze-Bergkamen, Beyond cell death – antiapoptotic Bcl-2 proteins regulate migration and invasion of colorectal cancer cells in vitro, PLoS One 8 (2013) e76446.
[34] J.D. Leverson, D.C. Phillips, M.J. Mitten, et al., Exploiting selective BCL-2 family inhibitors to dissect cell survival dependencies and define improved strategies for cancer therapy, Sci. Transl. Med (2015), https://doi.org/10.1126/SCITRANSLMED.AAA4642.
[35] C. Tse, A.R. Shoemaker, J. Adickes, et al., ABT-263: a potent and orally bioavailable Bcl-2 family inhibitor, Cancer Res 68 (2008) 3421–3428.
[36] J. Xiao, E. Glasgow, S. Agarwal, Zebrafish xenografts for drug discovery and personalized medicine, Trends Cancer 6 (2020) 569–579.
[37] M. Wadman, FDA no longer has to require animal testing for new drugs, Science (1979) 379 (2023) 127–128.
[38] I.H. Yang, J.Y. Jung, S.H. Kim, E.S. Yoo, N.P. Cho, H. Lee, J.Y. Lee, S.D. Hong, J. A. Shin, S.D. Cho, ABT-263 exhibits apoptosis-inducing potential in oral cancer cells by targeting C/EBP-homologous protein, Cell Oncol. 42 (2019) 357–368.
[39] C. Jensen, Y. Teng, Is it time to start transitioning from 2D to 3D cell culture, Front Mol. Biosci. (2020), https://doi.org/10.3389/FMOLB.2020.00033.
[40] J. Raitanen, B. Barta, M. Hacker, D. Georg, T. Balber, M. Mitterhauser, Comparison of radiation response between 2D and 3D cell culture models of different human cancer cell lines, Cells 12 (2023) 360.
[41] W. Wahbi, K. Korelin, M. Sieviläinen, P. Karihtala, T. Wilkman, J. Tarkkanen, T. Salo, A. Al-Samadi, Evaluation of in vitro and in vivo personalized cancer treatment assays for oral squamous cell carcinoma, Transl. Oncol. 33 (2023) 101677.
[42] B. Costa, S. Ferreira, V. Póvoa, et al., Developments in zebrafish avatars as radiotherapy sensitivity reporters - towards personalized medicine, EBioMedicine (2020), https://doi.org/10.1016/J.EBIOM.2019.11.039.
[43] A.W. Roberts, J.F. Seymour, J.R. Brown, et al., Substantial susceptibility of chronic lymphocytic leukemia to BCL2 inhibition: results of a phase I study of navitoclax in patients with relapsed or refractory disease, J. Clin. Oncol. 30 (2012) 488–496.
[44] C.N. Harrison, J.S. Garcia, T.C.P. Somervaille, et al., Addition of navitoclax to ongoing ruxolitinib therapy for patients with myelofibrosis with progression or suboptimal response: phase II safety and efficacy, J. Clin. Oncol. 40 (2022) 1671–1680.
[45] S. Khan, X. Zhang, D. Lv, et al., A selective BCL-XL PROTAC degrader achieves safe and potent antitumor activity, Nat. Med. 2019 25 12 (25) (2019) 1938–1947.